Advances in Basic and Applied Sciences 2 (2024) 46-52

Advances in Basic and Applied Sciences

journal homepage: https://abas.journals.ekb.eg/

Ionospheric Scintillation Prediction Model at Low Latitude Station Investigating a Machine Learning Technique

Hager M. Salah[1,2*], Daniel Okoh[3,4], M. Youssef [1], Ayman Mahrous[1,5]

[1]*Space Weather Monitoring Center Physics Department, Faculty of Science, Helwan University, Ain Helwan, Cairo 11795 Egypt*
[2] *Canadian International College in Cairo, Cairo, Egypt*
[3]*National Institute of Geophysics and Volcanology, Rome, Italy*
[4]*United Nations African Regional Centre for Space Science and Technology Education – English (UN-ARCSSTE-E), Obafemi Awolowo University Campus, Ile Ife, Nigeria*
[5]*Department of Space Environment, Institute of Basic and Applied Science, Egypt-Japan University of Science and Technology 21934 Alexandria, Egypt*

ARTICLE INFO

Article history:
Received 5 November 2023
Received in revised form 25 November 2023
Accepted 21 December 2023
Available online 31 January 2024

doi: 10.21608/ABAS.2023.245790.1037

Keywords: Ionospheric Scintillation, Equatorial ionization anomaly, GNSS, Machine Learning, Feedforward Backpropagation.

ABSTRACT

Ionospheric scintillation forecasting and modeling are vital for efficiently tracking satellites and navigation systems. Scintillations modulate the amplitude or phase of a signal waveform caused by abnormalities of the ionospheric electron density. These fluctuating signals can cause cycle slips, disconnect the receiver signal, and cause lock loss. In the current article, we predict the amplitude of scintillation (S4 index) using a machine-learning approach. A feedforward backpropagation technique was implemented. For further learning of models regarding the dynamics of the ionospheric F layer, we inserted foF2 and hmF2 parameters in the input layer neurons. The ground–based SCINDA data at Helwan, Egypt (29.86° N, 31.32° E) from 2009 to 2017 has been considered. The results show that predicted S4 values closely reflect observed S4 values for different conditions of the solar cycle 24, with a RMSE of 0.019 and regression of 0.659. The variations of ionospheric scintillation near the equatorial anomaly's northern peak have also been conducted during different levels of solar cycle 24 based on the ANN.

* **Corresponding author E-mail:** *hager.m.salah.92@gmail.com; hager.m.salah.92@science.helwan.edu.eg*

1. Introduction

Predicting ionospheric scintillations facilitates the implementation of essential mitigation measures to limit scintillation effects, enhancing satellite-based systems for communication and navigation [1]. Ionospheric scintillations are the fast amplitude and phase fluctuations of Global Navigation Satellite System (GNSS) signals induced by ionospheric electron density anomalies. They are more common after sunset and prevalent in equatorial low-latitude zones [2]. Scintillations are more prominent around the two peaks of the equatorial ionization anomaly (EIA), which can be seen between the latitudes of fifteen and twenty degrees north and south of the geomagnetic equator, where electron density reaches its maximum [3]. Amplitude scintillations are erratic changes in signal intensity that commonly generate pseudorange inaccuracies in GNSS transmissions. In the existence of scintillations, the number of satellites that can be seen necessary for precise positioning services decreases, resulting in position error [4]. This circumstance impairs the receiver's capacity to receive and track signals [5]. Since the scintillations are affected by the spatial and temporal features of the ionosphere and the space weather conditions[1], a precise selection of the prediction model is necessary because of the large datasets and many attributes. Although there are many techniques for predicting ionospheric conditions utilized by many authors, Artificial Neural Networks (ANN) have become a powerful tool for forecasting nonlinear ionospheric parameters [6]–[8]. The ANN approaches were discovered to be data-dependent, with performance improving as the sample size increased [9]. They apply a nonlinear function to determine the output as a weighted sum of the inputs to accurately predict future trends and behaviors for the given data. Several groups have modeled scintillation at low latitudes and the equator. Das et al.[10] predicted the occurrence probability of the ionospheric scintillation using backpropagation feedforward NN over Kolkata, which is located in the low latitude region of India during the solar cycle 23 from 1996 to 2006. They used the local time, the year's month number, and the month's average solar flux as the input variables of the developed model. A low-latitude scintillation activity forecasting model of VHF/UHF bands was developed by Redmon et al.[11] by considering observations near the geomagnetic equator from ionospheric sounder data. This model was based on ionospheric height fluctuations for the F2-maximum altitude but did not include any other physical characteristics linked to scintillation. De Lima et al.[12] have implemented a model using the classification and regression decision tree method for studying the correlation between the occurrence of the scintillation at the equatorial southern anomaly and the magnetic equator, which could be the basis for the ultimate creation of a prediction model appropriate for practical use. This model has used physical variables like solar flux, variations of the geomagnetic activity, the F2 layer's maximum height, the velocity of the F2 region, and amplitude scintillation. Taabu et al.[13] were presented with a feedforward NN trained with a backpropagation algorithm (Gradient-Descent algorithm) to investigate and forecast scintillation occurrences associated with the ionospheric irregularities over Kenya and Uganda using two years of data during solar cycle 24's ascending phase from VHF and SCINDA. The major disadvantage of this algorithm is the very slow convergence for adjusting the network weights. In another study, Atabati et al.[14] forecasted the amplitude scintillation parameter for a regression of 80% in the one-day forecasting for the GUAM station located in the low latitude region utilizing a hybrid NN and genetic algorithm technique.

In this work, an artificial neural network approach is represented for predicting the amplitude scintillation S4 index using ground-based data over the Helwan SCINDA station in the northern peak of the EIA. The Feedforward Backpropagation technique was investigated for training the ANN model. We also introduce an analysis of the ionospheric scintillation during different levels of solar cycle 24 based on the ANN.

2. Data analysis

GPS data was acquired for the purpose of this research utilizing a ground-based scintillation network and decision aid system (SCINDA) receiver at the low latitude region in Egypt (LAT: 29.86°N, LONG: 31.32°E, and MLAT 29.94°N). The receiver can track two signals simultaneously at 1580 MHz and 1230 MHz. The data set included all the data accessible from the station from 2009 to 2017, during different levels of solar cycle 24. The GSV4004 receiver tracks the amplitude scintillation at a 50 Hz sampling rate. In the present paper, we predict ionospheric scintillations using the S4 index. The S4 index was calculated for each 1 minute using the raw signal intensity's normalized standard deviation (SI) in each relevant epoch, as expressed in equation (1) [15].

$$S_4 = \sqrt{\frac{\langle SI^2 \rangle - \langle SI \rangle^2}{\langle SI \rangle^2}} \quad (1)$$

Multipath effects may be present in S4 calculations using this formula, especially at low elevation angles. In this investigation, we excluded satellite epochs at elevation angles less than 30° to reduce the multipath influence on the observation, as in the previous studies [2], [16]. Depending

on the model's requirements, S4 is utilized for time intervals varying from a few seconds to several hours. In our study, the S4 observations were calculated using the mean values for a five-minute time interval [13].

This study uses factors influencing the ionosphere that can affect the creation of ionospheric scintillation as inputs to our model. Among these parameters, the maximum height (hmF2) and F2' vertical critical frequency (foF2)[17] influence the F2 layer, the primary layer of the phenomenon of ionospheric scintillation [12]. Taking advantage of the International Reference Ionosphere models that can provide long-term data at our station that has no Ionosonde data [18], we used data from IRI-2016. It is primarily regarded as a reliable ionospheric model [19], collected from (https://ccmc.gsfc.nasa.gov/modelweb/models/iri2016_vitmo.php), offered by the Community Coordinated Modeling Center. This work additionally involves the use of solar and geomagnetic activity indices. This model uses number sunspots (SSN) and solar radio flux at 10.7cm wavelength (F10.7) as indicators of solar activity levels. The symmetric disturbances of the H-component (SYM-H)[20] and the international planetary geomagnetic index (Kp) indices are employed to determine the geomagnetic activity level. These indices were acquired from the National Aeronautics and Space Administration's OMNIWeb (https: //omniweb.gsfc.nasa.gov/).

3. Methodology

The artificial neural network (ANN) is a machine learning method that may be employed to model or predict linear and nonlinear variables like ionospheric scintillation. This method is less affected by noisy data and can handle large numbers of observations [21]. ANN comprises three layers: an input layer, one or more hidden layers, and an output layer. Each layer includes some nodes, or neurons, and the communication weights that link the nodes [22]. The input dataset is multiplied by the assigned weights, and the sum is fed into neurons. Each neuron has a transfer function that adopts this input value and determines the neuron's output value. Then, the difference between the predicted and actual output is calculated, and each neuron's weights and biases are adjusted to reduce the error, a technique called backpropagation. The process ends when the error rate between the model's output data and the target data entered as input into the model is as low as possible [23]. In order to train the feedforward neural network using backpropagation, use the Levenberg-Marquardt algorithm (trainlm). The trainlm uses optimization for updating weights and bias, which renders it the most productive backpropagation approach, with few iterations required to be more general [24].

The present model implements a typical fully linked feedforward NN with backpropagation. The prediction model comprises an input layer made up of a collection of inputs that feed the network's input patterns. The input layer is made up of the day number of the year (DOY), the universal time UT (HR), F10.7, SSN, Kp index, SYM-H index, IRI-foF2 parameter, and IRI-hmF2 parameter. DOY and HR were divided into two periodic components, as defined by equations (2) and (3), that provided for a numerically continuous pattern of data [25], [26]. After the input layer, there is one hidden layer. After that, an output layer generates the output results, the ROTI index, was used as the prediction model's output parameter.

$$DOY_s = \sin\left(\frac{2\pi \times DOY}{365.25}\right), and\ DOY_c = \cos\left(\frac{2\pi \times DOY}{365.25}\right) \quad (2)$$

$$HR_s = \sin\left(\frac{2\pi \times HR}{24}\right), and\ HR_c = \cos\left(\frac{2\pi \times HR}{24}\right) \quad (3)$$

The number of hidden layer neurons is crucial to ANN training. We varied the number of hidden layer neurons from 1 to 30. We calculated the error rate between the predicted scintillation values and the observed scintillation measurements to determine the number of hidden neurons. The parameter used is the root-mean-squared errors (RMSEs), described in equation (4)[27]. We identified the best model and number of hidden neurons with the lowest RMSE on the training and test datasets.

$$RMSE = \sqrt{\frac{\sum_{i=1}^{n}(S4obs_i - ANNpred_i)^2}{n}} \quad (4)$$

where $(S4obs_i)$ are the observed S4 measurements corresponding to the predicted S4 $(ANNpred_i)$, and (n) is the number of data points.

4. Results and Discussion

The first phase of the modeling entailed determining the inputs that will aid the network's learning of scintillation patterns of behavior throughout different circumstances. We built four different ANN models with different sets of input layer neurons. The models were used to investigate whether additional input layer neurons improved the performance of the networks. The different ANN models are described in Table 1. The first model comprises only the seasonal and daily variations, while we added the solar cycle variations to the second model. We added the geomagnetic variations and the ionospheric parameters to the third and fourth models, respectively.

For each model, the number of hidden layer neurons was changed from 1 to 30. Each trained neural network was then utilized to predict the S4 values for the validation and testing data sets. Testing and validating the model optimizes the model parameters to obtain an unbiased assessment of the final model fit to the training data.

Table 1. Different Neural Network models.

ANN models	Sets of Input layer neurons
ANN1	DOYs, DOYc, HRs, HRc
ANN2	DOYs, DOYc, HRs, HRc, SSN, F10.7
ANN3	DOYs, DOYc, HRs, HRc, SSN, F10.7, SYMH, Kp
ANN4	DOYs, DOYc, HRs, HRc, SSN, F10.7, SYMH, Kp, IRI-hmF2, IRI-foF2

We used 30% of the available dataset to validate and test the developed neural network model. For neural network predictions, the root mean square errors (RMSEs) were calculated using the corresponding measured S4 values as a basis for comparison. Figure 1 demonstrates how these calculated RMSEs compare to their respective counterparts for the four models. It strongly suggests that the fourth ANN model outperforms the other models. This is supported by the fact that the RMSEs of this model were typically lower. The selectedmodelnculude both F2 ionospheric characteristics a s inputs, hmF2, and foF2, which affect the scintillation behavior and consequently facilitate the network's learning of S4 index behavior during different phases of the solar cycle. The optimum performance of the selected model occurred at 8 neurons in the hidden layer, with an RMSE of 0.018. Therefore, the ANN algorithm designed for S4 index modeling to predict ionospheric scintillation is represented in Figure 2.

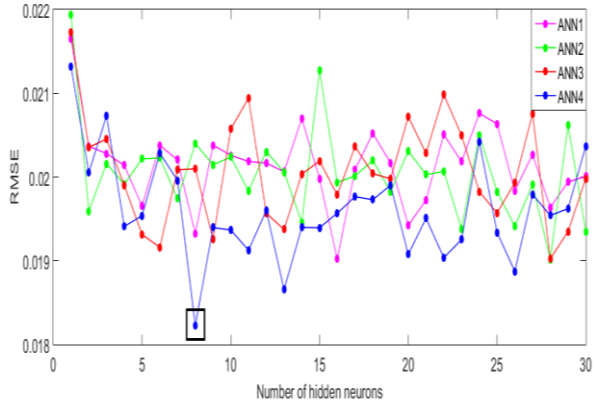

Figure 1. RMSEs of the four different neural network models were trained to test the validity of inputs and the number of hidden neurons.

The results of the predicted ionospheric scintillation on the S4 index using Helwan GPS-SCINDA data over the northern crest of the equatorial anomaly are shown in this section to evaluate the calibration process. Figure 3 compares predicted S4 values using ANN to similar ground-based data.

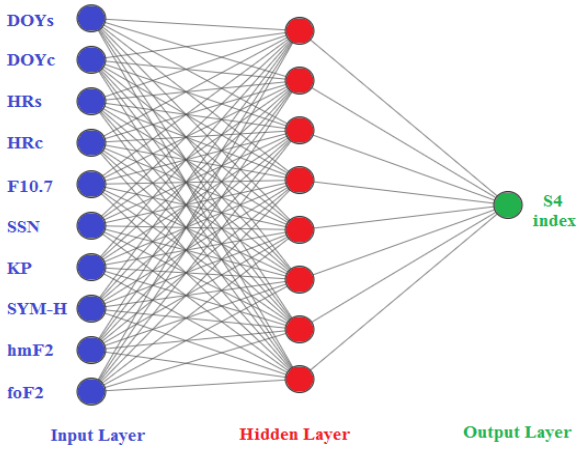

Figure 2. ANN algorithm designed for S4 index modeling.

Figure 3 a to c are, respectively, indicating the training, validation, and test data sets. Figure 3d represents all the data sets used for the prediction process. The correlation coefficient's values (R) and RMSE between the predicted ANN-S4 and observed Ground-S4s are illustrated in the figures. According to Figure 3 a to c, the correlation coefficients for the training, validation, and test data sets are 0.654, 0.670, and 0.675, respectively. On the other hand, for the training, validation, and test data sets, the RMSE values of the predictions from the observations are 0.019, 0.019, and 0.018, respectively. The obtained comparison of the RMSEs and correlation coefficients reveals that the values are not statistically different for the three data sets. This implies that the ANN approach used to predict S4 generalizes effectively; if not, it would outperform the validation and test data sets on the training data set. Effective generalization is required for neural networks since the networks must function well on data that wasn't utilized for training. In the case where all data sets are used, in Figure 3d, the modeled S4 and the observed S4 exhibit an intermediate correlation with a correlation coefficient of 0.659. This result proves that the predictions and measurements are related in a reasonable manner. The root-mean-square value of the differences is 0.019. This value represents that the artificial neural network model can be utilized to forecast the S4 index with a typical error of less than 0.019.

We compared the results of the diurnal variations of the S4 index estimated by the ANN model with the observations of corresponding data from the GPS-SCINDA station. The comparison contains the daily data for three months in three different seasons of the winter solstice (January), equinox (March), and summer solstice (July) in 2010 (minimum solar activity), 2012 (moderate solar activity), and 2014 (maximum solar activity). Figure 4 shows the S4 value over three days from each season during different solar activity levels to detect ionospheric scintillation. The days in January, March, and July are from the left column to the right. While the upper, second, and third panels introduced the years of 2010, 2012, and 2014, respectively. The observations of the

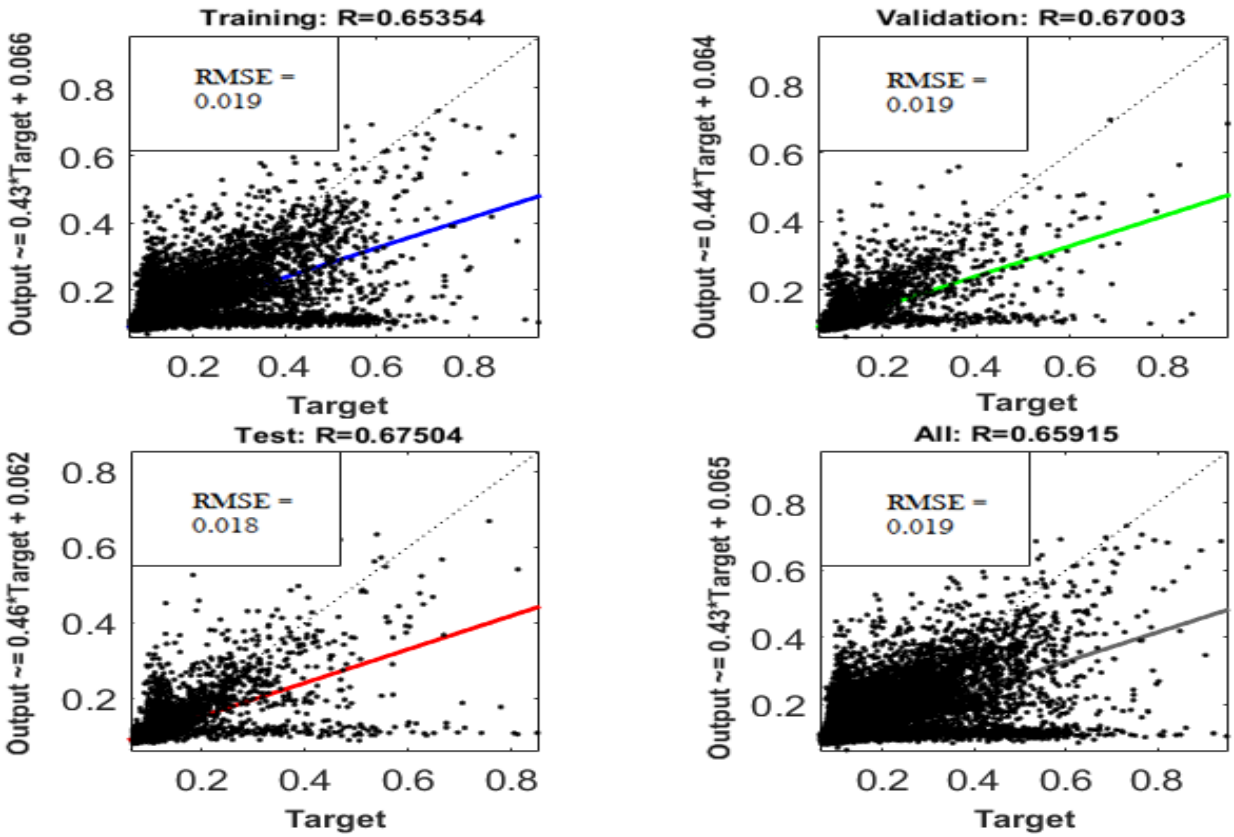

Figure 3. Plots of predicted S4s index versus corresponding observed Ground-S4s illustrated using (a) training data set, (b) validation data set, (c) test data set, and (d) all data sets.

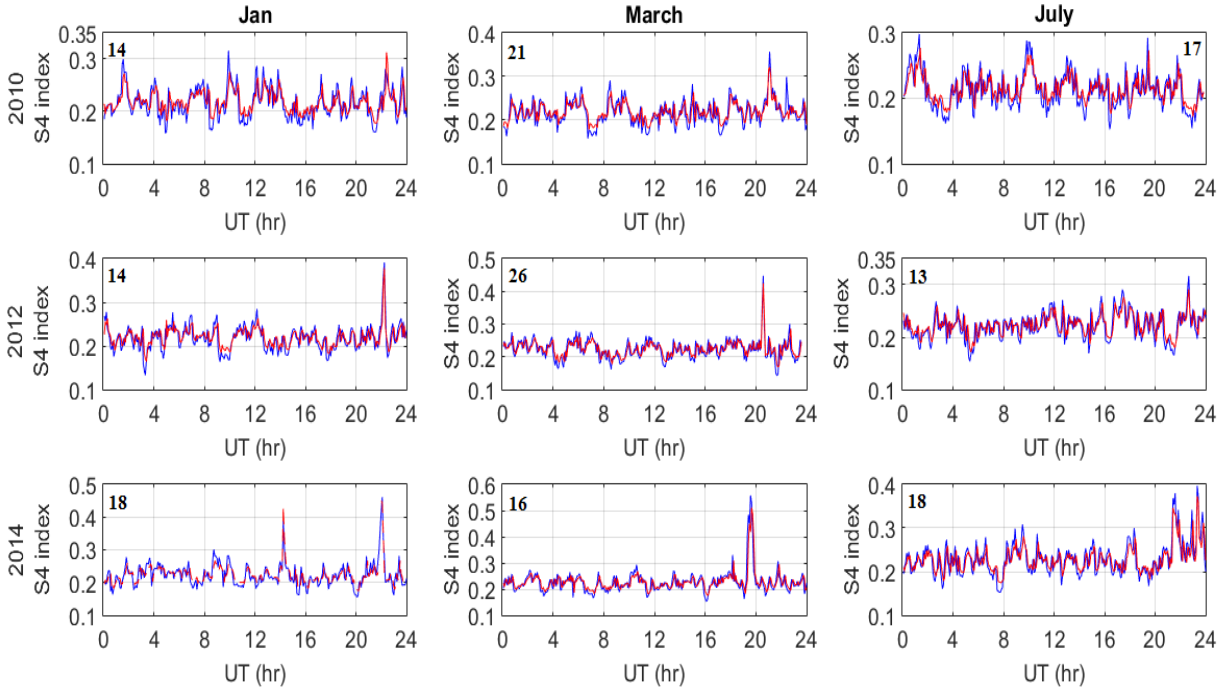

Figure 4. The ANN modeled and observed S4 in different solar activity levels during different seasons.

S4 index from GPS-SCINDA are represented in the blue line, while the predictions from the ANN model are described in the red line. The threshold value of S4 utilized in this figure to determine the presence of ionospheric scintillation was 0.2. The days were chosen because they provide a reliable depiction of ionospheric scintillation during various seasons and phases of the solar cycle.

As shown in Figure 4, the diurnal variation of the modeled ANN-S4 index pattern closely matches the daily GPS-S4 index trend for the different phases of the solar cycle 24. This comparison indicates that the ANN model provides a good, predicted value for the ROTI index. The ionospheric scintillation that occurred in 2014 (high solar activity) was higher than in 2012 (moderate solar activity) and 2010 (low solar activity). These results confirm that ionospheric scintillations occur at a higher rate during the peak of solar cycle 24, with the highest solar activity level. Furthermore, the S4 values for the days of the different seasons show that the ionospheric scintillation in March is higher than in January and July, respectively. The pattern of the scintillation occurrence during the current study period suggests that the amplitude scintillation over Helwan at L-band frequencies revealed peak occurrence during the equinoctial months rather than at the solstice. These results are confirmed by the previous studies [28], [29]. Paznukhov et al. [29]believed the alignment of the solar terminator and local geomagnetic field could sufficiently explain the seasonal climatology of scintillations observed by GPS in Africa.

Conclusions

In the current paper, we presented the prediction results of the ionospheric amplitude scintillation S4 index utilizing a feedforward backpropagation neural network approach with fair accuracy over a single station in the EIA's Northern peak. We found that the ionospheric parameters of the ionospheric F2-layer, hmF2 and foF2, presented better results for the modeling approaches. Our approach introduced a predicted pattern of the S4 index that closely matches the observed pattern by the ground-based data. The regression of the model is 0.659, while the RMSE value is 0.019. Our findings demonstrate that ionospheric scintillations occur at a higher rate during the peak of solar cycle 24 with the maximum solar activity level than in the moderate and low solar activity, respectively. Furthermore, the trend of scintillation occurrence indicated that amplitude scintillation increases during the equinoctial months rather than at the solstice.

Acknowledgment

The authors thank the SCINDA project and the SWMC Physics Department at Helwan University for providing the raw GPS-SCINDA data. We want to acknowledge the Community Coordinated Modeling Center for supplying IRI-2016 ionospheric parameters. We appreciate NASA OMNI-web for their assistance with the solar and geomagnetic indices.

References

[1] S. Basu, K. M. Groves, S. Basu, and P. J. Sultan, "Specification and forecasting of scintillations in communication/navigation links: current status and future plans," *J. Atmos. Solar-Terrestrial Phys.*, vol. 64, no. 16, pp. 1745–1754, Nov. 2002, doi: 10.1016/S1364-6826(02)00124-4.

[2] P. V. S. R. Rao, S. G. Krishna, K. Niranjan, and D. S. V. V. D. Prasad, "Study of spatial and temporal characteristics of L-band scintillations over the Indian low-latitude region and their possible effects on GPS navigation," *Ann. Geophys.*, vol. 24, no. 6, pp. 1567–1580, Jul. 2006, doi: 10.5194/ANGEO-24-1567-2006.

[3] E. V. Appleton, "The anomalous equatorial belt in the F2-layer," *J. Atmos. Terr. Phys.*, vol. 5, no. 1–6, pp. 348–351, Jan. 1954, doi: 10.1016/0021-9169(54)90054-9.

[4] M. Aquino *et al.*, "Improving the GNSS positioning stochastic model in the presence of ionospheric scintillation," *J. Geod.*, vol. 83, no. 10, pp. 953–966, Mar. 2009, doi: 10.1007/S00190-009-0313-6/METRICS.

[5] I. Sharp, K. Yu, and Y. J. Guo, "GDOP analysis for positioning system design," *IEEE Trans. Veh. Technol.*, vol. 58, no. 7, pp. 3371–3382, 2009, doi: 10.1109/TVT.2009.2017270.

[6] E. O. Oyeyemi, L. A. McKinnell, and A. W. V. Poole, "Neural network-based prediction techniques for global modeling of M(3000)F2 ionospheric parameter," *Adv. Sp. Res.*, vol. 39, no. 5, pp. 643–650, Jan. 2007, doi: 10.1016/J.ASR.2006.09.038.

[7] M. Tshisaphungo, J. B. Habarulema, and L. A. McKinnell, "Modeling ionospheric foF2 response during geomagnetic storms using neural network and linear regression techniques," *Adv. Sp. Res.*, vol. 61, no. 12, pp. 2891–2903, Jun. 2018, doi: 10.1016/J.ASR.2018.03.025.

[8] X. Bo *et al.*, "Prediction of ionospheric TEC over China based on long and short-term memory neural network," *Chinese J. Geophys.*, vol. 65, no. 7, pp. 2365–2377, Jul. 2022, doi: 10.6038/CJG2022P0557.

[9] M. A. Razi and K. Athappilly, "A comparative predictive analysis of neural networks (NNs), nonlinear regression and classification and regression tree (CART) models," *Expert Syst. Appl.*, vol. 29, no. 1, pp. 65–74, Jul. 2005, doi: 10.1016/J.ESWA.2005.01.006.

[10] A. Das, A. Das Gupta, and S. Ray, "Characteristics of L-band (1.5GHz) and VHF (244MHz) amplitude scintillations recorded at Kolkata during 1996-2006 and development of models for the occurrence probability of scintillations using neural network," *J. Atmos. Solar-Terrestrial Phys.*, vol. 72, no. 9–10, pp. 685–704, Jun. 2010, doi: 10.1016/j.jastp.2010.03.010.

[11] R. J. Redmon, D. Anderson, R. Caton, and T. Bullett, "A Forecasting Ionospheric Real-time Scintillation Tool (FIRST)," *Sp. Weather*, vol. 8, no. 12, Dec. 2010, doi: 10.1029/2010SW000582.

[12] G. R. T. De Lima *et al.*, "Correlation analysis between the occurrence of ionospheric scintillation at the magnetic equator and at the southern peak of the Equatorial Ionization Anomaly," *Sp. Weather*, vol. 12, no. 6, pp. 406–416, Jun. 2014, doi: 10.1002/2014SW001041.

[13] S. D. Taabu, F. M. D'Ujanga, and T. Ssenyonga, "Prediction of ionospheric scintillation using neural network over East African region during ascending phase of sunspot cycle 24," *Adv. Sp. Res.*, vol. 57, no. 7, pp. 1570–1584, Apr. 2016, doi: 10.1016/j.asr.2016.01.014.

[14] A. Atabati, M. Alizadeh, H. Schuh, and L. C. Tsai, "Ionospheric scintillation prediction on s4 and roti parameters using artificial neural network and genetic algorithm," *Remote Sens.*, vol. 13, no. 11, p. 2092, Jun. 2021, doi: 10.3390/rs13112092.

[15] S. Datta-Barua, P. H. Doherty, S. H. Delay, T. Dehel, and J. A. Klobuchar, "Ionospheric Scintillation Effects on Single and Dual Frequency GPS Positioning." pp. 336–346, Sep. 12, 2003. Accessed: Oct. 22, 2023. [Online]. Available: http://www.ion.org/publications/abstract.cfm?jp=p&articleID=5208

[16] J. S. Xu, J. Zhu, and L. Li, "Effects of a major storm on GPS amplitude scintillations and phase fluctuations at Wuhan in China," *Adv. Sp. Res.*, vol. 39, no. 8, pp. 1318–1324, Jan. 2007, doi: 10.1016/J.ASR.2007.03.004.

[17] H. M. Farid, R. Mawad, E. Ghamry, and A. Yoshikawa, "The Impact of Coronal Mass Ejections on the Seasonal Variation of the Ionospheric Critical Frequency f0F2," *Universe 2020, Vol. 6, Page 200*, vol. 6, no. 11, p. 200, Oct. 2020, doi: 10.3390/UNIVERSE6110200.

[18] D. Okoh *et al.*, "A regional GNSS-VTEC model over Nigeria using neural networks: A novel approach," *Geod. Geodyn.*, vol. 7, no. 1, pp. 19–31, Jan. 2016, doi: 10.1016/J.GEOG.2016.03.003.

[19] D. Bilitza, "International Reference Ionosphere 2000," *Radio Sci.*, vol. 36, no. 2, pp. 261–275, Mar. 2001, doi: 10.1029/2000RS002432.

[20] R. Mawad, M. Fathy, and E. Ghamry, "The Simultaneous Influence of the Solar Wind and Earth's Magnetic Field on the Weather," *Universe 2022, Vol. 8, Page 424*, vol. 8, no. 8, p. 424, Aug. 2022, doi: 10.3390/UNIVERSE8080424.

[21] S. S. Haykin, *Neural Networks and Learning Machines/Simon Haykin*. Prentice Hall: New York, NY, USA, 2009. Accessed: Oct. 22, 2023. [Online]. Available: https://books.google.com/books/about/Neural_Networks_and_Learning_Machines.html?id=KCwWOAAACAAJ

[22] R. (Russell) Beale and T. (Tom) Jackson, *Neural computing : an introduction*. CRC Press: London, UK, 1990. Accessed: Oct. 22, 2023. [Online]. Available: https://www.routledge.com/Neural-Computing---An-Introduction/Beale-Jackson/p/book/9780852742624

[23] M. Norgaard, *Neural Network Based System Identification Toolbox*. Department of Automation, Technical University of Denmark: Lyngby, Denmark, 2000. Accessed: Oct. 22, 2023. [Online]. Available: https://zbook.org/read/68845_neural-network-based-system-identification-toolbox.html

[24] J. B. Habarulema and L. A. McKinnell, "Investigating the performance of neural network backpropagation algorithms for TEC estimations using South African GPS data," *Ann. Geophys.*, vol. 30, no. 5, pp. 857–866, May 2012, doi: 10.5194/ANGEO-30-857-2012.

[25] J. B. Habarulema, L. A. McKinnell, and P. J. Cilliers, "Prediction of global positioning system total electron content using Neural Networks over South Africa," *J. Atmos. Solar-Terrestrial Phys.*, vol. 69, no. 15, pp. 1842–1850, Nov. 2007, doi: 10.1016/J.JASTP.2007.09.002.

[26] A. W. V. Poole and L. A. McKinnell, "On the predictability of foF2 using neural networks," *Radio Sci.*, vol. 35, no. 1, pp. 225–234, Jan. 2000, doi: 10.1029/1999RS900105.

[27] T. O. Hodson, "Root-mean-square error (RMSE) or mean absolute error (MAE): when to use them or not," *Geosci. Model Dev.*, vol. 15, no. 14, pp. 5481–5487, Jul. 2022, doi: 10.5194/GMD-15-5481-2022.

[28] F. M. D'Ujanga, P. Baki, J. O. Olwendo, and B. F. Twinamasiko, "Total electron content of the ionosphere at two stations in East Africa during the 24–25 October 2011 geomagnetic storm," *Adv. Sp. Res.*, vol. 51, no. 5, pp. 712–721, Mar. 2013,

[29] V. V. Paznukhov *et al.*, "Equatorial plasma bubbles and L-band scintillations in Africa during solar minimum," *Ann. Geophys.*, vol. 30, no. 4, pp. 675–682, Apr. 2012, doi: 10.5194/ANGEO-30-675-2012.